International Journal of Mathematical, Engineering and Management Sciences
Vol. 11, No. 2, 920-939, 2026
https://doi.org/10.33889/IJMEMS.2026.11.2.038

Computational Analysis of Two-parameter Integro-differential Problems in LCR-circuits

P. Antony Prince
Department of Mathematics,
Amrita School of Physical Science, Coimbatore, Amrita Vishwa Vidyapeetham, Tamil Nadu, India.
E-mail: p_antonyprince@cb.students.amrita.edu

Sekar Elango
Department of Mathematics,
Amrita School of Physical Science, Coimbatore, Amrita Vishwa Vidyapeetham, Tamil Nadu, India.
E-mail: e_sekar@cb.amrita.edu

L. Govindarao
Department of Mathematics,
Amrita School of Physical Science, Coimbatore, Amrita Vishwa Vidyapeetham, Tamil Nadu, India.
Corresponding author: l_govindarao@cb.amrita.edu

(Received on October 25, 2025; Revised on December 22, 2025 & January 24, 2026; Accepted on January 27, 2026)

Abstract
This paper solves the two-parameter singularly perturbed Fredholm integro-differential equations through the developed exponentially fitted operator method and monotone finite difference method. The differential component is determined computationally using a developed exponentially fitted operator approach and a monotone finite difference method. The composite trapezoidal rule evaluates the integral component on a uniform grid. The developed exponentially fitted operator method gives first-order convergence when the small parameter related to the perturbation is much smaller than the square of the second parameter, and second-order convergence when the square of the second parameter is much smaller than the perturbation parameter. In addition, the monotone finite difference method shows second-order convergence in both situations. Numerical results are included to support the theoretical findings of the proposed methods.

Keywords- Singular perturbation, Two-parameter, Fitted operator, Fredholm integral, Boundary layer.

1. Introduction

A differential equation formed by multiplying a tiny parameter with the highest derivative term is known as a singularly perturbed differential equation (SPDE) (Miller et al., 1996; Priyadarshana et al., 2024), various applications of SPDEs have been explored in recent studies (Govindarao and sekar, 2023; Deepika and Das, 2024; Hu et al., 2024).

Chow et al. (1978) used singular perturbation theory to power systems for ascertaining high-frequency oscillations. The authors illustrated that a mass-spring-damper system, characterized by a stiff spring, can be seen as a perturbation of a rigid rod. They simultaneously analyzed the intermachine oscillations in a multimachine system by considering it a perturbation from coherent machines oscillating nearly in unison. Electromechanical nonlinear models of power systems with singular perturbations are discussed in Peponides et al. (1982).

Integro-differential equations (IDEs) play an important role in numerous scientific fields, including engineering, physics, biology, chemistry, electrostatics, potential theory, finance, fluid dynamics, elasticity

theory, astronomy, economics, and heat-mass transfer (Rahman, 2007; Jalilian and Tahernezhad, 2019; Karaaslan 2021). In solving SPDEs, standard techniques based on equal step lengths produce erroneous results. They are unstable and unsatisfactory in the majority of circumstances (Izadi and Yuzbasi, 2022; Udupa et al., 2022; Mohapatra et al., 2023).

Specially IDE is used to form an LCR-circuit model (Thota et al., 2024) represents the equation

$$L\frac{dI(t)}{dt} + RI(t) + \frac{1}{C}\int_0^t I(\tau)\,d\tau = V_{in}(t).$$

In the above LCR circuit, consisting of an inductor (L), a capacitor (C), and a resistor (R) connected either in series or in parallel, the inductor stores energy in the form of a magnetic field and opposes changes in current, while the capacitor stores energy as an electric field and resists changes in voltage. The resistor dissipates electrical energy as heat and provides damping to the system. When an alternating voltage is applied, energy oscillates between the inductor and capacitor, producing a natural resonant behavior, whereas the resistor gradually suppresses these oscillations. In certain practical situations, the inductance value L is extremely small $(0 < L \ll 1)$. This small parameter multiplies the highest-order derivative in the governing differential equation of the LCR circuit, thereby introducing a singular perturbation. As a result, the original LCR model can be transformed into a singularly perturbed integro-differential equation, where the small inductance creates rapid transient layers in the solution and significantly influences the long-term dynamics. Recently, researchers have solved the LCR circuit numerically (Izadi and Kamandar, 2025; Izadi et al., 2025).

Based on the motivation behind, let us consider a class of two-parameter singularly perturbed Fredholm integro-differential equations (SPFIDEs) of the form,

$$\begin{cases} \mathfrak{L}y(x) \coloneqq (\mathfrak{L}_1 + \mathfrak{L}_2)y(x) = f(x), \quad x \in (0,1) = \Omega, \\ \qquad\qquad y(0) = A,\ y(1) = B, \end{cases} \tag{1}$$

where, $\mathfrak{L}_1 y(x) = \epsilon y''(x) + \mu a(x)y'(x) - b(x)y(x)$, $\mathfrak{L}_2 y(x) = \lambda \int_0^1 K(x,s)y(s)\,ds$, $0 < \epsilon, \mu \ll 1$, λ is a given parameter. The functions $a(x) \geq \alpha > 0$, $b(x) > \beta > 0$ and $f(x)$ are differentiable functions on $[0,1]$, $K(x,s)$ is a kernel function and A, B are constants, here the parameters ϵ and μ are tiny parameters. Once the parameter $\mu = 1$ the problem is a convection-diffusion type problem (Elango et al., 2025), in this situation, a boundary layer with width $O(\epsilon)$ emerges neighbouring to the edge $x = 0$. When $\mu = 0$, the problem transforms into a reaction-diffusion type problem (Amiraliyev et al., 2020; Elango et al., 2024; Govindarao et al., 2024), then the boundary layers occur near $x = 0$ and $x = 1$ with a width of $O(\sqrt{\epsilon})$.

In literature, Lange and Smith (1993) derived the existence and uniqueness of SPFIDEs. Cimen and Cakir (2021) used interpolating quadrature rules to compute SPFIDEs with boundary values. A computational solution for the non-linear first-order singularly perturbed Volterra integro-differential equations (VIDEs) developed by Sevgin (2014). Amiraliyev et al. (2018) established a method to calculate error estimates that are consistent across over various parameters for evaluating solutions of first-order SPFIDEs with uniform mesh and also established a differentiation method in second-order SPFIDEs with Shishkin mesh Amiraliyev et al. (2020). Durmaz and Amiraliyev (2021) solved the second-order reaction-diffusion SPFIDEs utilizing a fitted difference method on a Shishkin mesh. Subsequently, it achieved a non-optimal convergence rate of two. Elango et al. (2024) successfully solved the second-order reaction-diffusion and convection-diffusion SPFIDEs. Elango et al. (2025) using a central difference scheme applied for the second-order derivative portion and an integral component used by the composite trapezoidal rule with a non-uniform mesh. Later, they used an extrapolation method to achieve a higher-order convergence rate.

Govindarao et al. (2024) explored the reaction-diffusion SPFIDEs with non-local boundary conditions. The second-order derivative is constructed using a central difference method, while the integral component is determined using the composite trapezoidal rule. They succeeded in attaining a second-order convergence rate and later, by applying the extrapolation, a convergence rate of four is obtained. Priyadarshana et al. (2025) used adaptive grid-based moving mesh algorithms to solved singularly perturbed VIDE. Prince et al. (2025a) solved the system of SPFIDE with a uniform mesh. Prince et al. (2025b) used the Richardson extrapolation technique to obtain the higher-order convergence for SPFIDEs.

O'Malley (1967) investigated the nature of the two-parameter problem from an asymptotic perspective. Also, Priyadarshana and Mohapatra (2024) numerically solved 2D two-parameter convection-diffusion-reaction problems. Ansari et al. (2024) enhancing the accuracy for singularly perturbed parabolic convection–diffusion–reaction problems with two small parameters. Due to the tiny parameters ϵ and μ involving the differential equations, the standard finite difference is unsuitable for solving SPDE, which results in inaccurate solutions. Similarly, SPFIDEs cannot be effectively handled by standard finite difference methods when high accuracy is required. Our approach involves switching from the standard finite difference method to the Developed Exponentially Fitted Operator Method (DEFOM) and the Monotone Finite Difference Method (MFDM) for tiny parameters ϵ and μ.

DEFOM differs from the standard exponentially fitted operator (SEFO) technique. The SEFO method is effective for a single-layer as a convection-diffusion model problem. In this context, the boundary layer transitions from one side to a double side, necessitating a modification of the exponentially fitted operator difference method to accurately capture the behaviour of the moving boundary layer. MFDM is a finite difference approach recently employed by Amirali et al. (2024) to solve FIDEs; this approach is now extended to two-parameter SPFIDE.

This article aims to present a comparison of both (DEFOM and MFDM) methods error estimation and convergence rate. The DEFOM demonstrates first-order convergence when the perturbation's small parameter is significantly less than the square of the second parameter, and second-order convergence when the square of the second parameter is considerably smaller than the perturbation parameter. The monotone finite difference approach exhibits second-order convergence in both scenarios. **Table 1** illustrates the comparisons.

Table 1. Comparison of DEFOM and MFDM.

	Rate of convergence	
Method	$\epsilon \ll \mu^2$	$\mu^2 \ll \epsilon$
DEFOM	Order one	Order two
MFDM	Order two	Order two

As a result, the order of convergence is shown computationally.

The article is organized like this: Section 2 presents the stability of the two parameters SPFIDEs. Section 3 shows the numerical discretization of SPFIDEs with a DEFOM. Section 4 presents an error estimation of the DEFOM. Section 5 presents a numerical discretization of SPFIDEs with an MFDM. Section 6 shows an error estimation of the MFDM and Section 7 examines computational simulations.

***Notations*:** In this study, M stands for a positive constant that is independent of the mesh parameter (Δh) and perturbation parameters (ϵ, μ). The space of real-valued functions that are continuously differentiable

n times on [0,1] is represented by the letter $C^n([0,1])$, $\Re = \max_{x\in[0,1]} \int_0^1 |K(x,s)|ds$ and $y_i = y(x_i)$ indicate an approximation by the Y_i.

2. Stability

The solution of Equation (1) is related to the following characteristic equation

$$\epsilon\gamma^2(x) + \mu a(x)\gamma(x) - b(x) = 0.$$

The characteristic equation solutions are

$$\gamma_0(x) = \frac{-\mu a(x) - \sqrt{\mu^2(a(x))^2 + 4\epsilon b(x)}}{2\epsilon},$$
$$\gamma_1(x) = \frac{-\mu a(x) + \sqrt{\mu^2(a(x))^2 + 4\epsilon b(x)}}{2\epsilon},$$

these solutions characterize the layers at $x = 0$ and $x = 1$. Let

$$\mu_0 = -\max_{x\in[0,1]} \gamma_0(x) = \frac{1}{2\epsilon}\left[\sqrt{\mu^2(a(x))^2 + 4\epsilon b(x)} + \mu a(x)\right],$$
$$\mu_1 = \min_{x\in[0,1]} \gamma_1(x) = \frac{1}{2\epsilon}\left[\sqrt{\mu^2(a(x))^2 + 4\epsilon b(x)} - \mu a(x)\right].$$

The quantity $\gamma_0(x) < 0$ describes the boundary layer at $x = 0$, while $\gamma_1(x) > 0$ characterizes the layer at $x = 1$. The solutions of two external layers are characterized by $\mu^2 \ll \epsilon$ or $\mu^2/\epsilon \to 0$ as $\epsilon \to 0$, which implies that $\mu_0 \approx \mu_1 \approx \sqrt{\frac{b}{\epsilon}}$ and the layers are similar to the reaction-diffusion case $\mu = 0$ and $\epsilon \ll \mu^2$ i.e., $\frac{\epsilon}{\mu^2} \to 0$ as $\mu \to 0$, the boundary layer attains only at $x = 0$. In this case, $\mu_0 \approx \min_{\{x\in[0,1]\}} \frac{\mu\alpha}{\epsilon}$ and $\mu_1 \approx 0$.

Lemma 2.1 Suppose that $a(x), b(x), f(x) \in C^2[0,1]$, $\frac{\partial^n K(x,s)}{\partial x^n} \in C[0,1], (n = 0,1,2)$ and $|\lambda| \leq \frac{\beta}{\Re}$. Then Equation (1) satisfies the following bounds

$$\| y \|_\infty \leq M,$$
$$\left|y^{(r)}(x)\right| \leq M\left\{1 + \frac{1}{\epsilon^r}\left(e^{-\mu_0 x} + e^{-\mu_1(1-x)}\right)\right\}, \quad (r = 1,2,3,4),\ x \in [0,1].$$

Proof. The proof of Lemma 2.1 is in a similar manner as in Durmaz et al. (2022).

Lemma 2.2 For all integer w on a fixed mesh, it gives

$$\lim_{\epsilon\to 0} \max_{1\leq i\leq N-1} \left(\frac{e^{-\frac{M}{\sqrt{\epsilon}}x_i}}{\epsilon^{\frac{w}{2}}}\right) = 0 \text{ and } \lim_{\epsilon\to 0} \max_{1\leq i\leq N-1} \left(\frac{e^{-\frac{M}{\sqrt{\epsilon}}(1-x_i)}}{\epsilon^{\frac{w}{2}}}\right) = 0,$$

where, $x_i = i(\Delta h)$.

Proof. One can find proof of this lemma in Prince et al. (2025a).

3. Numerical Discretization for DEFOM

On $[0,1]$, the uniform mesh step Δh is used to discretise the interval. Here, $\Delta h := \frac{1}{N}$ such that $x_i = i(\Delta h), 0 \le i \le N$, where, N is a number of finite mesh points.

For each mesh point of Equation (1) becomes

$$\mathfrak{L}^{(\Delta h)}y(x_i) := \mathfrak{L}_1^{(\Delta h)}y(x_i) + \mathfrak{L}_2^{(\Delta h)}y(x_i) = f(x_i),\ \ i = 0,1,2,\cdots N \tag{2}$$

where,

$$\mathfrak{L}_1^{(\Delta h)}y(x_i) = \epsilon y''(x_i) + \mu a(x_i)y'(x_i) - b(x_i)y(x_i),$$
$$\mathfrak{L}_2^{(\Delta h)}y(x_i) = \lambda\int_0^1 K(x_i,s)y(s)\,ds,\ \ i = 0,1,\cdots,N.$$

For any mesh function y_i, define backward, forward and central difference operators as follows:

$$D_x^- y_i = \frac{y_i - y_{i-1}}{\Delta h},\quad D_x^+ y_i = \frac{y_{i+1} - y_i}{\Delta h},\quad D_x^c y_i = \frac{y_{i+1} - y_{i-1}}{2(\Delta h)},$$
$$\delta_x^2 y_i \equiv D_x^+ D_x^- y_i = \frac{y_{i-1} - 2y_i + y_{i+1}}{(\Delta h)^2}.$$

Let's apply the exponentially fitted operator for the differential part $\mathfrak{L}_1^{(\Delta h)}$, then

$$\mathfrak{L}_1^{(\Delta h)}y(x_i) = \epsilon\sigma(\rho)\delta_x^2 y_i + \mu a(x_i)D_x^c y_i - b(x_i)y_i,$$

where, $\sigma(\rho) = \frac{\rho a(x)}{2}\ coth\left(\frac{\rho a(x)}{2}\right)$.

For the left boundary layer,

$$\sigma(\rho)_l = \frac{\rho a(0)}{2}\ coth\left(\frac{\rho a(0)}{2}\right) \tag{3}$$

For the right boundary layer,

$$\sigma(\rho)_r = \frac{\rho a(1)}{2}\ coth\left(\frac{\rho a(1)}{2}\right) \tag{4}$$

where, $\rho = \frac{\mu(\Delta h)}{\epsilon}$.

Equation (3) and Equation (4) combine to form a variable fitting factor,

$$\sigma_i := \sigma(\rho)_i = \frac{\rho a(x_i)}{2}\ coth\left(\frac{\rho a(x_i)}{2}\right),$$

Equation (2) contains both left and right layers so the finite difference scheme $\mathfrak{L}_1^{(\Delta h)}y(x_i)$ is

$$\mathfrak{L}_1^{(\Delta h)}y(x_i)\ = \epsilon\sigma(\rho)_i\delta_x^2 y_i + \mu a(x_i)D_x^c y_i - b(x_i)y_i.$$

Therefore, the discretization becomes

$$\mathfrak{L}_1^{(\Delta h)}y(x_i) = \left(\frac{\epsilon\sigma(\rho)_i}{(\Delta h)^2} - \frac{\mu a(x_i)}{2(\Delta h)}\right)y_{i-1} + \left(\frac{-2\epsilon\sigma(\rho)_i}{(\Delta h)^2} - b(x_i)\right)y_i + \left(\frac{\epsilon\sigma(\rho)_i}{(\Delta h)^2} + \frac{\mu a(x_i)}{2(\Delta h)}\right)y_{i+1}, \text{ for } i = 1,2,\ldots N.$$

The integral component is evaluated using the composite trapezoidal rule (Kress, 1998) then,

$$\mathfrak{L}_2^{(\Delta h)} y(x_i) = \lambda \sum_{j=0}^{N} \theta_j \, (\Delta h) \, K(x_i, s_j) \, y(s_j),$$

where, $\theta_j = \begin{cases} \frac{1}{2}, & \text{for } j = 0, N, \\ 1, & \text{for } j = 1,2,\cdots, N-1. \end{cases}$

4. Error Estimation for DEFOM

Here, $y(x_i)$ is the continuous solution of Equation (1) and Y_i is the computational solution of Equation (2). The solution is split into the differential part and the integral part, the error estimation follows like

$$|y(x_i) - Y_i| \quad = \left|\left(y_D(x_i) + y_I(x_i)\right) - \left(Y_i^D + Y_i^I\right)\right|,$$

where, $y_D(x_i), y_I(x_i)$ represent the continuous solutions of the differential part and integral part, similarly Y_i^D, Y_i^I represent the numerical solutions of the differential part and integral part. The following lemma shows the error estimate of the differential part.

Lemma 4.1 Let $y_D(x_i)$ and Y_i^D be the functions of $\mathfrak{L}_1$ and $\mathfrak{L}_1^{(\Delta h)}$, then the bound

$$\max_{0 \le i \le N} \left| y_D(x_i) - Y_i^D \right| \le M(\Delta h).$$

Proof.

$$\begin{aligned}
\left(\mathfrak{L}_1 - \mathfrak{L}_1^{(\Delta h)}\right) y_i \quad &= [\epsilon y_i'' + \mu a(x_i) y_i' - b(x_i) y_i] - [\epsilon \sigma_i \delta_x^2 y_i + \mu a(x_i) D_x^c y_i - b(x_i) y_i], \\
&= \left[\epsilon \frac{d^2}{dx^2} + \mu a(x_i) \frac{d}{dx}\right] y_i - [\epsilon \sigma_i \delta_x^2 + \mu a(x_i) D_x^c] y_i, \\
&= -\epsilon(\sigma_i - 1)\delta_x^2 y_i + \epsilon\left(\frac{d^2}{dx^2} - \delta_x^2\right) y_i + \mu a(x_i)\left(\frac{d}{dx} - D_x^c\right) y_i,
\end{aligned}$$

$$\left|\left(\mathfrak{L}_1 - \mathfrak{L}_1^{(\Delta h)}\right) y_i\right| \le |\epsilon(\sigma_i - 1)\delta_x^2 y_i| + \left|\epsilon\left(\frac{d^2}{dx^2} - \delta_x^2\right) y_i\right| + \left|\mu a(x_i)\left(\frac{d}{dx} - D_x^c\right) y_i\right|,$$

$$= \left|\epsilon\left(\rho \frac{a(x_i)}{2} \, coth\left(\rho \frac{a(x_i)}{2}\right) - 1\right)\delta_x^2 y_i\right| + \left|\epsilon\left(\frac{d^2}{dx^2} - \delta_x^2\right) y_i\right| + \left|\mu a(x_i)\left(\frac{d}{dx} - D_x^c\right) y_i\right|.$$

Let M be a constant utilising hyperbolic cotangent power series expansions, then $|z \, coth(z) - 1| \le Mz^2$, for $z \le 1$. Since $coth(z) \to 1$ as $z \to \infty$. So that $|coth(z) - 1| \le Mz$ for $z \ge 0$. Then combine these inequalities

$$z \, coth(z) - 1 \le \frac{Mz^2}{z+1}.$$

Now

$$\epsilon\left(\frac{\rho a(x_i)}{2} \, coth\left(\frac{\rho a(x_i)}{2}\right) - 1\right) \le M\epsilon \frac{\rho^2}{\rho+1} = M \frac{\mu^2 (\Delta h)^2}{(\mu(\Delta h)) + \epsilon}.$$

Utilising the Taylor series expansion, then the following bounds are

$$|\delta_x^2 y_i| \le M \parallel y^{(2)}(\eta_i) \parallel,$$

$$\left|\left(\frac{d}{dx} - D_x^0\right) y_i\right| \le M(\Delta h)^2 \parallel y^{(3)}(\eta_i) \parallel,$$

$$\left|\left(\frac{d^2}{dx^2} - \delta_x^2\right) y_i\right| \le M(\Delta h)^2 \parallel y^{(4)}(\eta_i) \parallel, \text{ for } \eta_i \in (x_{i-1}, x_{i+1}).$$

Apply the bounds, then it implies

$$\left|\left(\mathfrak{L}_1 - \mathfrak{L}_1^{(\Delta h)}\right) y_i\right| \le M\left(\frac{\mu^2(\Delta h)^2}{(\mu(\Delta h)) + \epsilon}\right) \parallel y^{(2)}(\eta_i) \parallel + M\epsilon(\Delta h)^2 \parallel y^{(4)}(\eta_i) \parallel + M\mu(\Delta h)^2 \parallel y^{(3)}(\eta_i) \parallel.$$

Now this spilt into two cases

Case (i): $\mu^2 \ll \epsilon$

$$\left|\left(\mathfrak{L}_1 - \mathfrak{L}_1^{(\Delta h)}\right) y_i\right| \le M\left(\frac{\mu^2(\Delta h)^2}{\epsilon}\right) \parallel y^{(2)}(\eta_i) \parallel + M\epsilon(\Delta h)^2 \parallel y^{(4)}(\eta_i) \parallel + M\mu(\Delta h) \parallel y^{(3)}(\eta_i) \parallel.$$

By applying Lemma 2.1 and Lemma 2.2 with $\epsilon \to 0$, then it follows that

$$\left|\left(\mathfrak{L}_1 - \mathfrak{L}_1^{(\Delta h)}\right) y_i\right| \le M(\Delta h)^2 \tag{5}$$

Case (ii): $\epsilon \ll \mu^2$

$$\left|\left(\mathfrak{L}_1 - \mathfrak{L}_1^{(\Delta h)}\right) y_i\right| \le M\left(\frac{\mu^2(\Delta h)^2}{(\mu(\Delta h)) + \epsilon}\right) \parallel y^{(2)}(\eta_i) \parallel + M\epsilon(\Delta h)^2 \parallel y^{(4)}(\eta_i) \parallel + M\mu(\Delta h) \parallel y^{(3)}(\eta_i) \parallel,$$

$$\le M\left(\frac{(\Delta h)^2}{(\Delta h) + \epsilon/\mu^2}\right) \parallel y^{(2)}(\eta_i) \parallel + M\epsilon(\Delta h)^2 \parallel y^{(4)}(\eta_i) \parallel + M\mu(\Delta h) \parallel y^{(3)}(\eta_i) \parallel.$$

By applying Lemma 2.1 and Lemma 2.2 with $\mu \to 0$ then it follows that

$$\left|\left(\mathfrak{L}_1 - \mathfrak{L}_1^{(\Delta h)}\right) y_i\right| \le M(\Delta h) \tag{6}$$

Combine Equation (5) and Equation (6), then

$$\left|\left(\mathfrak{L}_1 - \mathfrak{L}_1^{(\Delta h)}\right) y_i\right| \le \begin{cases} M(\Delta h)^2, & \text{if } \mu^2 \ll \epsilon, \\ M(\Delta h), & \text{if } \epsilon \ll \mu^2. \end{cases}$$

Then it implies

$$\max_{0 \le i \le N} \left|y_D(x_i) - Y_i^D\right| \le \begin{cases} M(\Delta h)^2, & \text{if } \mu^2 \ll \epsilon, \\ M(\Delta h), & \text{if } \epsilon \ll \mu^2. \end{cases}$$

Lemma 4.2 Let $y_I(x_i)$ and Y_i^I be the functions of $\mathfrak{L}_2$ and $\mathfrak{L}_2^{(\Delta h)}$, then the bound is

$$\text{i.e,} \qquad \sup_{0 \le x \le 1} \left|y_I(x_i) - Y_i^I\right| \le M(\Delta h)^2.$$

Proof. This lemma can be proven by the method of (Ref. pp 299, Kress, 1998).
Let $|\lambda| < \frac{\alpha}{\Re}$,

$$\left|(\mathfrak{Q}_2 - \mathfrak{Q}_2^{(\Delta h)})y_i\right| = \left|\lambda\int_0^1 K(x_i,s)y(s)\,ds - \lambda\sum_{j=0}^{N}\theta_j\,(\Delta h)\,K(x_i,s_j)\,y(s_j)\right|,$$
$$\leq \frac{1}{12}|\lambda|(\Delta h)^2 \max_{0\leq x_i,s\leq 1}\left|\frac{\partial^2}{\partial s^2}[K(x_i,s)y(s)]\right|,$$
$$\leq M(\Delta h)^2.$$

It follows that

$$\max_{0\leq x\leq 1}\left|y_I(x_i) - Y_i^I\right| \leq M(\Delta h)^2.$$

Theorem 4.3 Let $y(x_i)$ and Y_i be the solutions of Equation (1) and Equation (2), then

$$\sup_{0<\epsilon,\mu<1}\max_{0\leq i\leq N}|y(x_i) - Y_i| \leq \begin{cases} M(\Delta h)^2, & \text{if } \mu^2 \ll \epsilon, \\ M(\Delta h), & \text{if } \epsilon \ll \mu^2. \end{cases}$$

Proof.

$$|y(x_i) - Y_i| \leq \left|y_D(x_i) - Y_i^D\right| + \left|y_I(x_i) - Y_i^I\right|.$$

By using the Lemma 4.1 and Lemma 4.2 it follows. If $\mu^2 \ll \epsilon$, then

$$|y(x_i) - Y_i| \leq M(\Delta h)^2 + M(\Delta h)^2,$$
$$\leq M(\Delta h)^2.$$

Similarly, if $\epsilon \ll \mu^2$, then

$$|y(x_i) - Y_i| \leq M(\Delta h) + M(\Delta h)^2,$$
$$\leq M(\Delta h).$$

The above inequalities imply

$$\sup_{0<\epsilon,\mu<1}\max_{0\leq i\leq N}|y(x_i) - Y_i| \leq \begin{cases} M(\Delta h)^2, & \text{if } \mu^2 \ll \epsilon, \\ M(\Delta h), & \text{if } \epsilon \ll \mu^2. \end{cases}$$

5. Numerical Discretization for MFDM

Using the finite difference relation for Equation (2),

$$\epsilon y''(x_i) = \epsilon\delta_x^2 y_i + \epsilon\mathcal{R}_i^1,$$
$$\mu y'(x_i) = \mu D_x^c y_i + \mu\mathcal{R}_i^2,$$

where,

$$\epsilon\mathcal{R}_i^1 = \epsilon\frac{-(\Delta h)^2}{12}y^{(4)}(\eta_i),$$
$$\mu\mathcal{R}_i^2 = \mu\frac{-(\Delta h)^2}{6}y^{(3)}(\eta_i), \quad \eta_i \in (x_{i+1}, x_{i-1}).$$

For the integral term applying the composite trapezoidal rule, then

$$\mathfrak{L}_2^{(\Delta h)} y(x_i) = \lambda \sum_{j=0}^{N} \theta_j \, (\Delta h) \, K(x_i, s_j) \, y(s_j) + \mathcal{R}_i^3,$$

where,

$$\theta_j = \begin{cases} \frac{1}{2}, & \text{for } j = 0, N, \\ 1, & \text{for } j = 1,2, \cdots, N-1, \end{cases}$$

$$\mathcal{R}_i^3 = \frac{-1}{12} \lambda (\Delta h)^2 \left(\frac{\partial^2}{\partial s^2} [K(x_i, s) y(s)] \right).$$

Now Equation (2) follows

$$\begin{aligned} \mathfrak{L}^{(\Delta h)} y(x_i) \coloneqq \epsilon \delta_x^2 y_i + \mu a(x_i) D_x^c y_i - b(x_i) y(x_i) \\ + \lambda \textstyle\sum_{j=0}^{N} \theta_j \, (\Delta h) \, K(x_i, s_j) \, y(s_j) = f(x_i) - \left(\epsilon \mathcal{R}_i^1 + \mu \mathcal{R}_i^2 + \mathcal{R}_i^3 \right) \end{aligned} \tag{7}$$

Use the relation

$$D_x^c y_i = D_x^+ y_i - \frac{(\Delta h)}{2} \delta_x^2 y_i,$$

then Equation (7) implies

$$\begin{aligned} \left(\epsilon - \tfrac{\mu a(x_i)(\Delta h)}{2} \right) \delta_x^2 y_i + \mu a(x_i) D_x^+ y_i - b(x_i) y(x_i) \\ + \lambda \textstyle\sum_{j=0}^{N} \theta_j \, (\Delta h) \, K(x_i, s_j) \, y(s_j) = f(x_i) - \overline{\mathcal{R}}_i \end{aligned} \tag{8}$$

where, $\overline{\mathcal{R}}_i = \epsilon \mathcal{R}_i^1 + \mu \mathcal{R}_i^2 + \mathcal{R}_i^3$.

In Equation (8), let

$$\epsilon - \tfrac{\mu a(x_i)(\Delta h)}{2} = \epsilon \left(1 - \tfrac{\mu a(x_i)(\Delta h)}{2\epsilon} \right),$$

apply the equality conditions

$$1 - T = \tfrac{1}{1+T} - \tfrac{T^2}{1+T} \equiv \tfrac{1}{1+T} + O(T^2), \; T > 0,$$

then Equation (8) implies

$$\chi_i \delta_x^2 y_i + \mu a(x_i) D_x^+ y_i - b(x_i) y(x_i) + \lambda \sum_{j=0}^{N} \theta_j \, (\Delta h) \, K(x_i, s_j) \, y(s_j) = f(x_i) - R_i,$$

where,

$$R_i = \overline{\mathcal{R}_i} + \epsilon \mathcal{R}_i^4,$$

$$\mathcal{R}_i^4 = -\frac{(\mu a(x_i)(\Delta h)/2\epsilon)^2}{1 + (\mu a(x_i)(\Delta h)/2\epsilon)} \delta_x^2,$$

$$\chi_i = \frac{\epsilon}{1 + (\mu a(x_i)(\Delta h)/2\epsilon)}.$$

Thereby the proposed difference scheme for Equation (1)

$$\mathfrak{L}^{(\Delta h)}y(x_i) := \begin{cases} \chi_i \delta_x^2 v_i + \mu a(x_i) D_x^+ v_i - b(x_i)v(x_i) + \lambda \sum_{j=0}^{N} \theta_j\,(\Delta h)\, K(x_i, s_j)\, v(s_j) = f(x_i), \\ v_0 = A, \quad v_N = B. \end{cases} \tag{9}$$

6. Error Estimation for MFDM

To analyze the convergence of this approach, consider that the error function $\kappa_i = v_i - y_i, 0 \le i \le N$ is the solution of the subsequent discrete problem

$$\mathfrak{L}^{(\Delta h)}y(x_i) := \begin{cases} \chi_i \delta_x^2 \kappa_i + \mu a(x_i) D_x^+ \kappa_i - b(x_i)\kappa(x_i) + \lambda \sum_{j=0}^{N} \theta_j\,(\Delta h)\, K(x_i, s_j)\, \kappa(s_j) = R_i, \\ \kappa_0 = 0, \quad \kappa_1 = 0. \end{cases}$$

where, y_i and v_i be the solution of Equation (8) and Equation (9) respectively and R_i denotes the truncation error.

Theorem 6.1 If $a(x), b(x), f(x) \in C([0,1])$, $K(x,s) \in C^2([0,1]^2)$ and $y(x) \in C^4[0,1]$, then the truncation error R_i is satisfies the inequality

$$\| R \| \le M(\Delta h)^2.$$

Proof. The proof follows a similar approach as in Amirali et al. (2024),

Case (i): $\epsilon \ll \mu^2$ and $\mu \to 0$ then $\epsilon/\mu^2 \to 0$

$$\begin{aligned} |\epsilon \mathcal{R}_i^1| &\le \epsilon \frac{(\Delta h)^2}{12} \| y^{(4)}(\eta_i) \|, \\ &\le M\epsilon \frac{(\Delta h)^2}{12}\left\{1 + \frac{1}{\epsilon^4}\left(e^{-\mu_0 \eta_i} + e^{-\mu_1(1-\eta_i)}\right)\right\}, \\ |\mu \mathcal{R}_i^2| &\le \mu \frac{(\Delta h)^2}{6} \| y^{(3)}(\eta_i) \|, \\ &\le M\mu \frac{(\Delta h)^2}{6}\left\{1 + \frac{1}{\epsilon^3}\left(e^{-\mu_0 \eta_i} + e^{-\mu_1(1-\eta_i)}\right)\right\}, \\ |\mathcal{R}_i^3| &\le |\lambda| \frac{(\Delta h)^2}{12}\left\{\| \frac{\partial^2 K}{\partial s^2} \| \| y(\eta_i) \| + 2 \| \frac{\partial K(x,s)}{\partial s} \| \| y'(\eta_i) \| + \| K(\eta_i, s) \| \| y^{(2)}(\eta_i) \|\right\}, \\ &\le M \frac{(\Delta h)^2}{12}\left\{1 + \frac{1}{\epsilon^2}\left(e^{-\mu_0 \eta_i} + e^{-\mu_1(1-\eta_i)}\right)\right\} \end{aligned}$$

and

$$\begin{aligned} |\epsilon \mathcal{R}_i^4| &\le \left| \frac{\epsilon \left(\frac{\mu a(x_i)(\Delta h)}{2\epsilon}\right)^2}{1 + \left(\frac{\mu a(x_i)(\Delta h)}{2\epsilon}\right)} \right| \| y^{(2)}(\eta_i) \|, \\ &\le \frac{\mu^2 \frac{\| a \|^2 (\Delta h)^2}{4}}{\epsilon + \mu \| a \| \left(\frac{\Delta h}{2}\right)} \| y^{(2)}(\eta_i) \|, \\ &\le \frac{\mu \frac{\| a \|^2 (\Delta h)^2}{4}}{\frac{\epsilon}{\mu} + \| a \| \left(\frac{\Delta h}{2}\right)}\left\{1 + \frac{1}{\epsilon^2}\left(e^{-\mu_0 \eta_i} + e^{-\mu_1(1-\eta_i)}\right)\right\}. \end{aligned}$$

Now apply $\mu \to 0$ and Lemma 2.2, then
$|R_i| \leq M(\Delta h)^2$ (10)

Case(ii): $\mu^2 \ll \epsilon$ and $\epsilon \to 0$ then $\mu^2/\epsilon \to 0$,

$$|\epsilon \mathcal{R}_i^4| \leq \left| \frac{\epsilon \left(\frac{\mu a(x_i)(\Delta h)}{2\epsilon}\right)^2}{1+\left(\frac{\mu a(x_i)(\Delta h)}{2\epsilon}\right)} \right| \| y^{(2)}(\eta_i) \|,$$

$$\leq \left| \frac{a(x_i)^2(\Delta h)^2 \left(\frac{\mu^2}{4\epsilon}\right)}{1+\left(\frac{\mu a(x_i)(\Delta h)}{2\epsilon}\right)} \right| \left\{1 + \frac{1}{\epsilon^2}\left(e^{-\mu_0 \eta_i} + e^{-\mu_1(1-\eta_i)}\right)\right\}.$$

Now apply $\epsilon \to 0$ and Lemma 2.2, then
$|R_i| \leq M(\Delta h)^2$ (11)

Following that, combine Equation (10) and Equation (11)

$$\| R \| \leq M(\Delta h)^2.$$

7. Computational Simulations

This section computationally verifies the theoretical results gained. The maximum absolute errors and the convergence order in the maximum norm are provided for the test problems.

Example 7.1 *Consider the two-parameter SPFIDE example*

$$\begin{cases} \epsilon y''(x) + \mu y'(x) - y(x) + \int_0^1 y(s)\, ds = f(x), \\ y(0) = 1, \quad y(1) = 0, \end{cases}$$

where,

$$f(x) = \frac{1}{2} + \sqrt{4\epsilon + \mu^2}\, csch\left(\frac{\sqrt{4\epsilon+\mu^2}}{2\epsilon}\right)\left[\mu \cosh\left(\frac{\mu}{2\epsilon}\right) - \mu \cosh\left(\frac{\sqrt{4\epsilon+\mu^2}}{2\epsilon}\right) + \sinh\left(\frac{\mu}{2\epsilon}\right)\right] - x.$$

The exact solution of this Example 7.1 is

$$y(x) = (x+\mu) + \frac{\left((1-\mu) + (1+\mu)e^{-\theta_2}\right)e^{\theta_1 x} - \left((1+\mu) + (1-\mu)e^{\theta_1}\right)e^{-\theta_2(1-x)}}{1 - e^{\frac{\sqrt{\mu^2+4\epsilon}}{\epsilon}}},$$

where, $\theta_{1,2} = \frac{-\mu \pm \sqrt{\mu^2+4\epsilon}}{2\epsilon}$.

Example 7.2 *Consider the two-parameter SPFIDE example*

$$\begin{cases} \epsilon y''(x) + \mu(1+x)y'(x) - 2y(x) + \frac{1}{2}\int_0^1 xy(s)\, ds = 16x^2(1-x)^2, \\ y(0) = -1, \quad y(1) = 1. \end{cases}$$

The error estimate for Example 7.1 is

$$e_{\epsilon}^{N} = \max_{i} \| y(x_i) - Y_i \|,$$

where, $y(x_i)$ is the exact solution and Y_i is the approximation solution.

In Example 7.2 does not possess an exact solution. Consequently, an error estimate is followed by a double mesh error analysis. The error obtained by

$$e_{\epsilon}^{N} = \max_{i} \left| y_i^{\epsilon,N} - \tilde{y}_i^{\epsilon,2N} \right|,$$

where, $y_i^{\epsilon,N}$, $\tilde{y}_i^{\epsilon,2N}$ are the approximate solutions of the related method with the mesh points N and $2N$ respectively.

The rate of convergence is $p_{\epsilon}^{N} = \log_2 \left(\frac{e_{\epsilon}^{N}}{e_{\epsilon}^{2N}} \right)$.

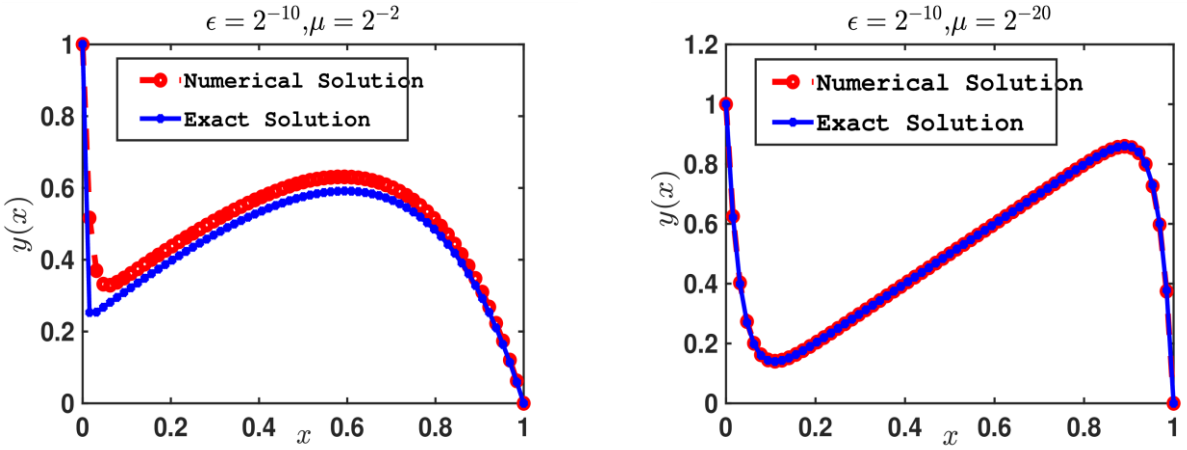

Figure 1. DEFOM numerical solution and exact solution of example 7.1 for $N = 64$.

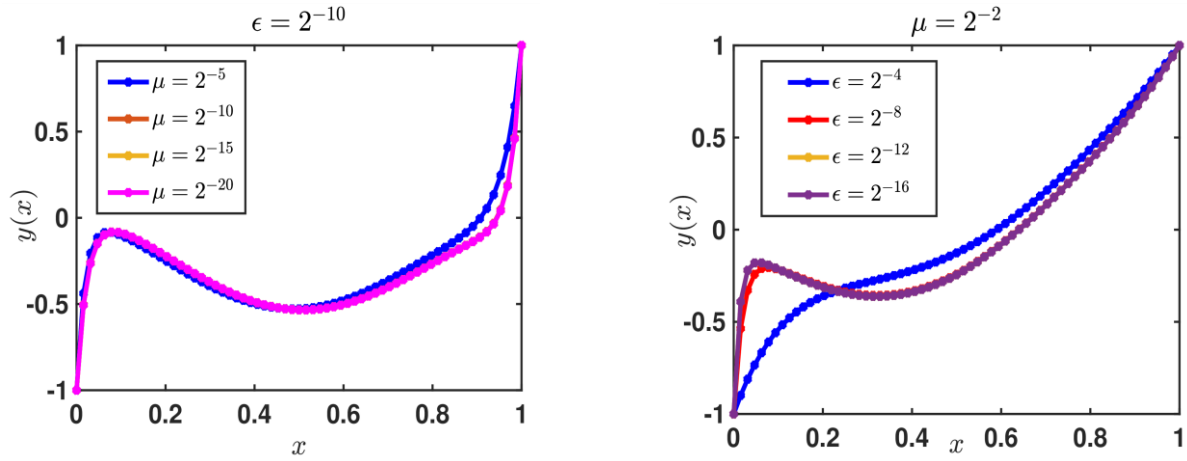

Figure 2. Numerical solution of example 7.2 with various μ and ϵ for $N = 64$.

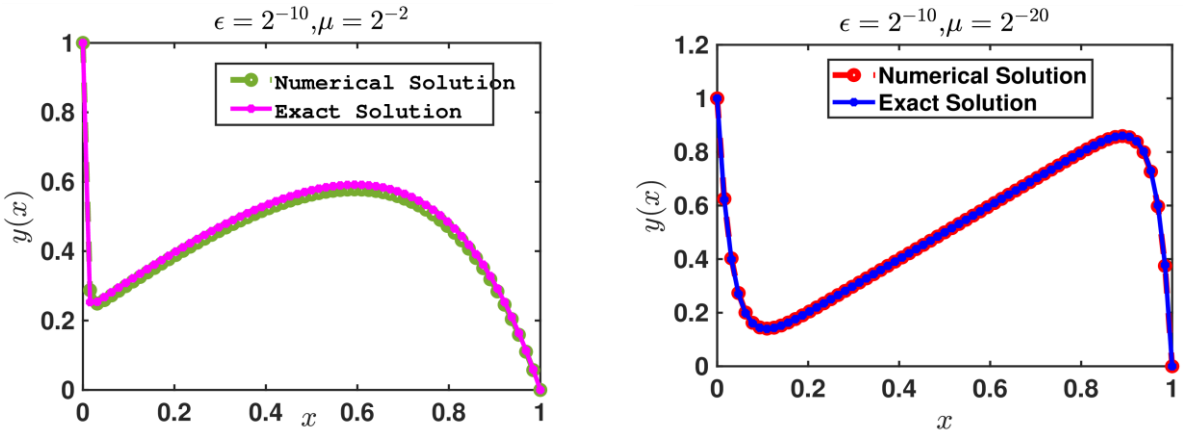

Figure 3. MFDM numerical solution and exact solution of example 7.1 for $N = 64$.

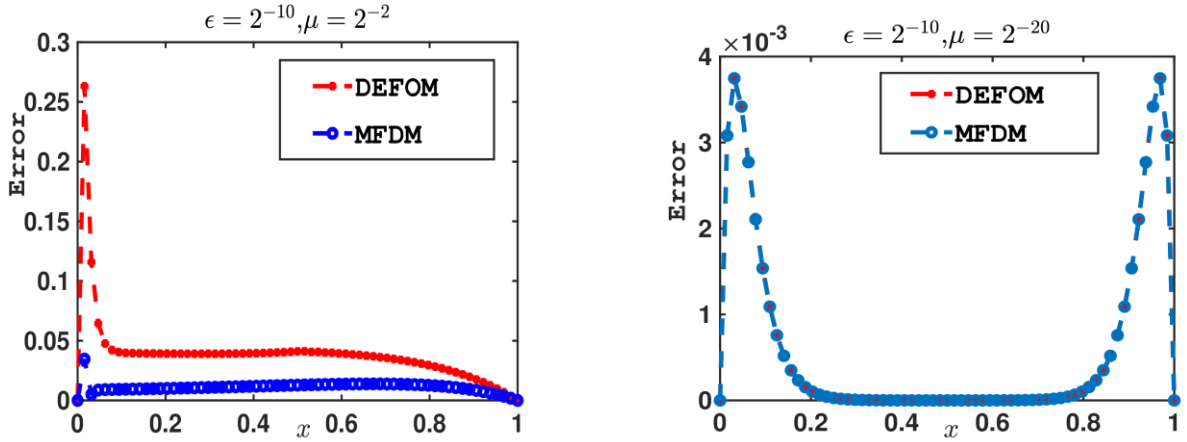

Figure 4. Comparsion error plot of example 7.1 for $N = 64$.

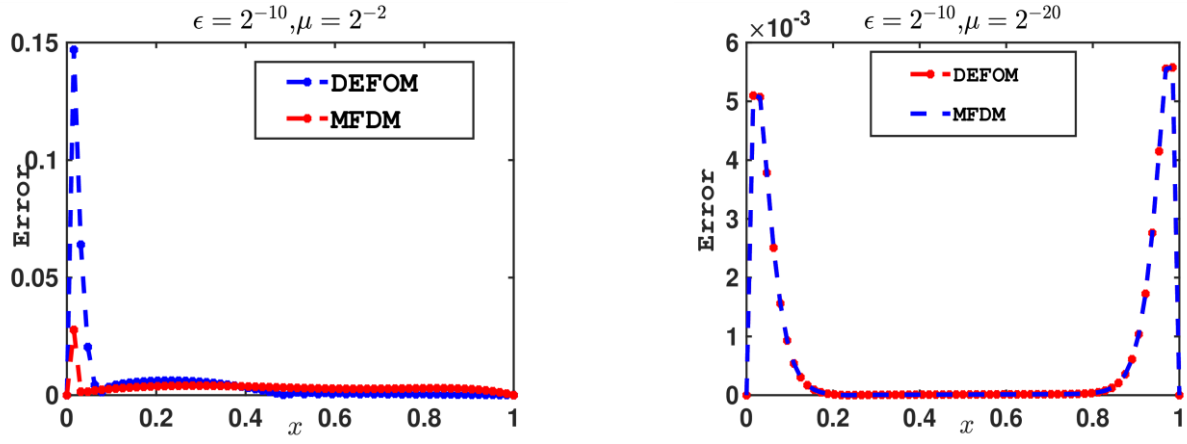

Figure 5. Comparsion error plot of example 7.2 for $N = 64$.

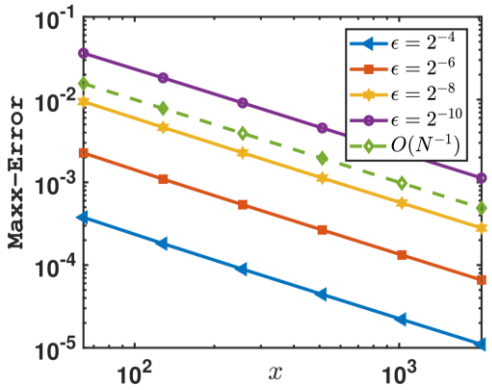

Figure 6. Log-log plot with corresponding values of $\epsilon \ll \mu^2$ of example 7.1 with DEFOM.

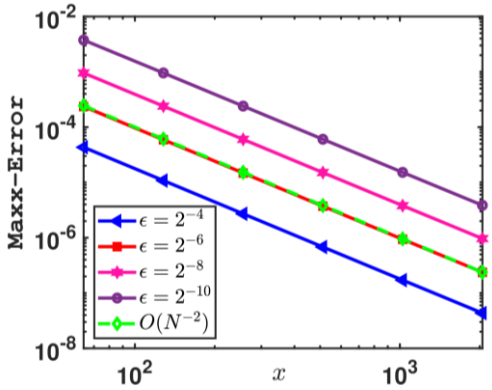

Figure 7. Log-log plot with corresponding values of $\mu^2 \ll \epsilon$ of example 7.1 with DEFOM.

Table 2. Maximum absolute error and convergence rate of example 7.1.

		Number of intervals N and $\mu = 2^{-7}$					
	$\epsilon \downarrow$	64	128	256	512	1024	2048
DEFOM	2^{-4}	3.7723e-4	1.8147e-4	8.9126e-5	4.4196e-5	2.2012e-5	1.0985e-5
		1.0557	**1.0258**	**1.0119**	**1.0056**	**1.0027**	**1.0014**
MFDM		4.5633e-5	1.1412e-5	2.8538e-6	7.1346e-7	1.7837e-7	4.4629e-8
		1.9995	**1.9996**	**2.0000**	**2.0000**	**1.9988**	**2.0208**
DEFOM	2^{-6}	2.2637e-3	1.0919e-3	5.3610e-4	2.6561e-4	1.3220e-4	6.5948e-5
		1.0519	**1.0262**	**1.0132**	**1.0066**	**1.0033**	**1.0017**
MFDM		2.5618e-4	6.4147e-5	1.6046e-5	4.0117e-6	1.0030e-6	2.5075e-7
		1.9977	**1.9992**	**1.9999**	**2.0000**	**1.9999**	**2.0015**
DEFOM	2^{-8}	9.4519e-3	4.6137e-3	2.2734e-3	1.1279e-3	5.6167e-4	2.8026e-4
		1.0347	**1.0210**	**1.0113**	**1.0058**	**1.0030**	**1.0015**
MFDM		1.0824e-3	2.7268e-4	6.8276e-5	1.7079e-5	4.2703e-6	1.0677e-6
		1.9890	**1.9977**	**1.9991**	**1.9998**	**1.9999**	**2.0002**
DEFOM	2^{-10}	3.6391e-2	1.8287e-2	9.1110e-3	4.5353e-3	2.2615e-3	1.1291e-3
		0.9927	**1.0052**	**1.0064**	**1.0039**	**1.0022**	**1.0011**
MFDM		4.7248e-3	1.2157e-3	3.0670e-4	7.6840e-5	1.9232e-5	4.8095e-6
		1.9585	**1.9869**	**1.9969**	**1.9984**	**1.9995**	**1.9998**
DEFOM	2^{-12}	1.2089e-1	6.9015e-2	3.5569e-2	1.7955e-2	8.9968e-3	4.5010e-3
		0.8087	**0.9563**	**0.9862**	**0.9969**	**0.9992**	**0.9998**
MFDM		2.1008e-2	5.9832e-3	1.5663e-3	3.9751e-4	1.0010e-4	2.5100e-5
		1.8120	**1.9336**	**1.9783**	**1.9895**	**1.9957**	**1.9979**

Table 3. Maximum absolute error and convergence rate of example 7.1.

		Number of intervals N and $\epsilon = 2^{-10}$					
	$\mu \downarrow$	64	128	256	512	1024	2048
DEFOM	2^{-4}	1.8853e-1	1.0434e-1	5.5253e-2	2.8346e-2	1.4347e-2	7.2201e-3
		0.8536	**0.9171**	**0.9629**	**0.9823**	**0.9907**	**0.9954**
MFDM		2.4055e-2	8.0660e-3	2.4460e-3	6.6882e-4	1.7539e-4	4.4883e-5
		1.5764	**1.7214**	**1.8707**	**1.9310**	**1.9664**	**1.9828**
DEFOM	2^{-6}	6.8645e-2	3.5431e-2	1.7896e-2	8.9706e-3	4.4887e-3	2.2449e-3
		0.9541	**0.9854**	**0.9964**	**0.9989**	**0.9996**	**0.9998**
MFDM		6.2106e-3	1.6216e-3	4.1196e-4	1.0372e-4	2.6007e-5	6.5111e-6
		1.9373	**1.9769**	**1.9898**	**1.9957**	**1.9979**	**1.9990**
DEFOM	2^{-8}	1.9784e-2	9.4989e-3	4.6302e-3	2.2799e-3	1.1307e-3	5.6296e-4
		1.0585	**1.0367**	**1.0221**	**1.0118**	**1.0061**	**1.0031**
MFDM		4.1645e-3	1.0598e-3	2.6665e-4	6.6805e-5	1.6707e-5	4.1775e-6
		1.9743	**1.9909**	**1.9969**	**1.9995**	**1.9997**	**2.0000**
DEFOM	2^{-10}	7.4630e-3	2.9955e-3	1.2999e-3	6.0164e-4	2.8921e-4	1.4179e-4
		1.3169	**1.2045**	**1.1114**	**1.0568**	**1.0284**	**1.0141**
MFDM		3.8342e-3	9.7483e-4	2.4476e-4	6.1256e-5	1.5319e-5	3.8304e-6
		1.9757	**1.9938**	**1.9984**	**1.9995**	**1.9998**	**2.0000**
DEFOM	2^{-18}	3.7613e-3	9.6003e-4	2.4295e-4	6.1756e-5	1.5923e-5	4.2226e-6
		1.9701	**1.9824**	**1.9760**	**1.9554**	**1.9150**	**1.8423**
MFDM		3.7474e-3	9.5266e-4	2.3918e-4	5.9860e-5	1.4969e-5	3.7425e-6
		1.9759	**1.9938**	**1.9985**	**1.9996**	**1.9999**	**2.0000**
DEFOM	2^{-20}	3.7507e-3	9.5444e-4	2.4011e-4	6.0330e-5	1.5206e-5	3.8615e-6
		1.9744	**1.9910**	**1.9927**	**1.9883**	**1.9774**	**1.9558**
MFDM		3.7472e-3	9.5260e-4	2.3917e-4	5.9856e-5	1.4968e-5	3.7422e-6
		1.9759	**1.9938**	**1.9985**	**1.9996**	**1.9999**	**1.9999**

Table 4. Maximum absolute error and convergence rate of example 7.1.

		Number of intervals N and $\mu = 2^{-20}$					
	$\epsilon \downarrow$	64	128	256	512	1024	2048
DEFOM	2^{-4}	4.3228e-5	1.0820e-5	2.7101e-6	6.7984e-7	1.7112e-7	4.3349e-8
		1.9983	**1.9973**	**1.9951**	**1.9902**	**1.9810**	**1.9326**
MFDM		4.3176e-6	1.0795e-6	2.6988e-7	6.7476e-8	1.6870e-8	4.2132e-9
		1.9999	**2.0000**	**1.9999**	**1.9999**	**2.0015**	**1.6068**
DEFOM	2^{-6}	2.3595e-4	5.9109e-5	1.4810e-5	3.7173e-6	9.3641e-7	2.3765e-7
		1.9970	**1.9968**	**1.9942**	**1.9890**	**1.9783**	**1.9570**
MFDM		4.3191e-5	1.0801e-5	2.7010e-6	6.7525e-7	1.6883e-7	4.2206e-8
		1.9995	**1.9997**	**2.0000**	**1.9998**	**2.0001**	**1.9693**
DEFOM	2^{-8}	9.5349e-4	2.3963e-4	6.0091e-5	1.5086e-5	3.8016e-6	9.6539e-7
		1.9924	**1.9956**	**1.9939**	**1.9886**	**1.9774**	**1.9554**
MFDM		2.3573e-4	5.8996e-5	1.4754e-5	3.6891e-6	9.2228e-7	2.3058e-7
		1.9984	**1.9995**	**1.9997**	**2.0000**	**1.9999**	**2.0000**
DEFOM	2^{-10}	3.7507e-3	9.5444e-4	2.4011e-4	6.0330e-5	1.5206e-5	3.8615e-6
		1.9744	**1.9910**	**1.9927**	**1.9883**	**1.9774**	**1.9558**
MFDM		9.5258e-4	2.3916e-4	5.9855e-5	1.4968e-5	3.7422e-6	9.3561e-7
		1.9938	**1.9985**	**1.9996**	**1.9999**	**1.9999**	**1.9997**
DEFOM	2^{-12}	1.4099e-2	3.7542e-3	9.5631e-4	2.4106e-4	6.0806e-5	1.5444e-5
		1.9090	**1.9730**	**1.9881**	**1.9871**	**1.9772**	**1.9557**
MFDM		3.7472e-3	9.5260e-4	2.3917e-4	5.9856e-5	1.4968e-5	3.7422e-6
		1.9759	**1.9938**	**1.9985**	**1.9996**	**1.9999**	**1.9999**

Table 5. Maximum absolute error and convergence rate of example 7.2.

		Number of intervals N and $\mu = 2^{-7}$					
	$\epsilon \downarrow$	64	128	256	512	1024	2048
DEFOM	2^{-4}	1.6555e-4	7.4300e-5	4.2258e-5	2.2538e-5	1.1631e-5	5.9070e-6
		1.1558	**0.8141**	**0.9069**	**0.9544**	**0.9775**	**0.9888**
MFDM		2.3271e-5	5.8178e-6	1.4542e-6	3.6354e-7	9.0882e-8	2.2660e-8
		2.0000	**2.0002**	**2.0001**	**2.0001**	**2.0038**	**2.0840**
DEFOM	2^{-6}	7.2628e-4	2.8738e-4	1.4876e-4	8.1133e-5	4.2253e-5	2.1548e-5
		1.3376	**0.9500**	**0.8746**	**0.9412**	**0.9715**	**0.9860**
MFDM		1.0454e-4	2.6162e-5	6.5423e-6	1.6357e-6	4.0892e-7	1.0223e-7
		1.9986	**1.9996**	**1.9999**	**2.0000**	**2.0000**	**2.0020**
DEFOM	2^{-8}	2.8736e-3	1.1306e-3	5.7705e-4	3.1460e-4	1.6378e-4	8.3504e-5
		1.3458	**0.9703**	**0.8752**	**0.9418**	**0.9718**	**0.9861**
MFDM		4.3786e-4	1.0978e-4	2.7485e-5	6.8727e-6	1.7183e-6	4.2958e-7
		1.9959	**1.9979**	**1.9997**	**1.9999**	**2.0000**	**2.0001**
DEFOM	2^{-10}	1.0307e-2	4.3547e-3	2.1089e-3	1.1608e-3	6.0615e-4	3.0941e-4
		1.2430	**1.0461**	**0.8613**	**0.9374**	**0.9701**	**0.9854**
MFDM		1.7603e-3	4.4535e-4	1.1171e-4	2.7957e-5	6.9927e-6	1.7484e-6
		1.9828	**1.9952**	**1.9985**	**1.9993**	**1.9998**	**1.9999**
DEFOM	2^{-12}	3.2922e-2	1.6041e-2	7.4631e-3	3.7290e-3	1.9649e-3	1.0063e-3
		1.0373	**1.1039**	**1.0010**	**0.9243**	**0.9654**	**0.9834**
MFDM		7.6720e-3	2.0428e-3	5.2306e-4	1.3169e-4	3.3024e-5	8.2656e-6
		1.9091	**1.9655**	**1.9899**	**1.9955**	**1.9983**	**1.9992**

Table 6. Maximum absolute error and convergence rate of example 7.2.

		Number of intervals N and $\epsilon = 2^{-10}$					
	$\mu \downarrow$	64	128	256	512	1024	2048
DEFOM	2^{-4}	5.6967e-2	3.0887e-2	1.6704e-2	8.6957e-3	4.4440e-3	2.2476e-3
		0.8831	**0.8868**	**0.9418**	**0.9684**	**0.9835**	**0.9914**
MFDM		1.8118e-2	6.2916e-3	1.9896e-3	5.4966e-4	1.4464e-4	3.7111e-5
		1.5260	**1.6610**	**1.8558**	**1.9261**	**1.9626**	**1.9811**
DEFOM	2^{-6}	1.6176e-2	7.5615e-3	3.6834e-3	1.9415e-3	9.9448e-4	5.0306e-4
		1.0971	**1.0376**	**0.9238**	**0.9652**	**0.9832**	**0.9919**
MFDM		1.0032e-2	2.7841e-3	7.2766e-4	1.8560e-4	4.6840e-5	1.1765e-5
		1.8493	**1.9359**	**1.9711**	**1.9864**	**1.9932**	**1.9967**
DEFOM	2^{-8}	7.6113e-3	2.8396e-3	1.1034e-3	5.9538e-4	3.2338e-4	1.6811e-4
		1.4225	**1.3637**	**0.8901**	**0.8806**	**0.9438**	**0.9729**
MFDM		6.4623e-3	1.7423e-3	4.4078e-4	1.1056e-4	2.7677e-5	6.9219e-6
		1.8911	**1.9828**	**1.9952**	**1.9981**	**1.9994**	**1.9998**
DEFOM	2^{-10}	5.7078e-3	1.7544e-3	5.3706e-4	1.8188e-4	6.9062e-5	4.0611e-5
		1.7020	**1.7078**	**1.5621**	**1.3970**	**0.7660**	**0.8937**
MFDM		5.7355e-3	1.5749e-3	3.9788e-4	9.9735e-5	2.4966e-5	6.2426e-6
		1.8646	**1.9849**	**1.9962**	**1.9981**	**1.9998**	**1.9999**
DEFOM	2^{-14}	5.4987e-3	1.4917e-3	3.6588e-4	9.4747e-5	2.5167e-5	7.0216e-6
		1.8821	**2.0275**	**1.9492**	**1.9126**	**1.8416**	**1.7278**
MFDM		5.5825e-3	1.5386e-3	3.8869e-4	9.7539e-5	2.4410e-5	6.1040e-6
		1.8593	**1.9849**	**1.9946**	**1.9985**	**1.9997**	**1.9999**
DEFOM	2^{-16}	5.5578e-3	1.5253e-3	3.8235e-4	9.4459e-5	2.2994e-5	5.9321e-6
		1.8654	**1.9961**	**2.0171**	**2.0384**	**1.9546**	**1.9140**
MFDM		5.5787e-3	1.5370e-3	3.8829e-4	9.7447e-5	2.4386e-5	6.0981e-6
		1.8598	**1.9849**	**1.9944**	**1.9985**	**1.9996**	**1.9999**

Table 7. Maximum absolute error and convergence rate of example 7.2.

		Number of intervals N and $\mu = 2^{-20}$					
	$\epsilon \downarrow$	64	128	256	512	1024	2048
DEFOM	2^{-4}	1.0441e-4	2.6122e-5	6.5293e-6	1.6311e-6	4.0708e-7	1.0141e-7
		1.9989	**2.0003**	**2.0010**	**2.0025**	**2.0051**	**2.0116**
MFDM		2.3571e-5	5.8930e-6	1.4730e-6	3.6824e-7	9.2058e-8	2.2952e-8
		1.9999	**2.0002**	**2.0001**	**2.0000**	**2.0039**	**2.0970**
DEFOM	2^{-6}	4.2360e-4	1.0642e-4	2.6613e-5	6.6496e-6	1.6596e-6	4.1350e-7
		1.9929	**1.9996**	**2.0008**	**2.0024**	**2.0049**	**2.0100**
MFDM		1.0443e-4	2.6134e-5	6.5351e-6	1.6340e-6	4.0851e-7	1.0212e-7
		1.9986	**1.9996**	**1.9998**	**2.0000**	**2.0000**	**2.0016**
DEFOM	2^{-8}	1.5716e-3	3.9695e-4	9.9570e-5	2.4895e-5	6.2139e-6	1.5478e-6
		1.9852	**1.9952**	**1.9998**	**2.0023**	**2.0052**	**2.0107**
MFDM		4.2369e-4	1.0647e-4	2.6636e-5	6.6609e-6	1.6653e-6	4.1634e-7
		1.9926	**1.9990**	**1.9996**	**1.9999**	**2.0000**	**2.0000**
DEFOM	2^{-10}	5.5763e-3	1.5358e-3	3.8780e-4	9.7232e-5	2.4286e-5	6.0495e-6
		1.8603	**1.9856**	**1.9958**	**2.0013**	**2.0052**	**2.0111**
MFDM		1.5720e-3	3.9713e-4	9.9662e-5	2.4941e-5	6.2368e-6	1.5593e-6
		1.9849	**1.9945**	**1.9985**	**1.9997**	**1.9999**	**2.0000**
DEFOM	2^{-12}	1.9373e-2	5.5404e-3	1.5252e-3	3.8493e-4	9.6424e-5	2.4035e-5
		1.8060	**1.8610**	**1.9863**	**1.9971**	**2.0042**	**2.0110**
MFDM		5.5776e-3	1.5365e-3	3.8817e-4	9.7419e-5	2.4379e-5	6.0963e-6
		1.8600	**1.9849**	**1.9944**	**1.9986**	**1.9996**	**1.9999**

Table 8. Maximum absolute error example 7.1.

Parameters	N	Shishkin mesh	DEFOM	MFDM
$\epsilon = 2^{-10}, \mu = 2^{-20}$	64	3.7486e-3	3.7507e-3	9.5258e-4
	128	9.5329e-4	9.5444e-4	2.3916e-4
	256	2.3952e-4	2.4011e-4	5.9855e-5
	512	6.0031e-5	6.0330e-5	1.4968e-5
	1024	1.5056e-5	1.5206e-5	3.7422e-6
	2048	3.7861e-6	3.8615e-6	9.3561e-7

Table 9. Maximum absolute error example 7.2.

Parameters	N	Finite difference method	DEFOM	MFDM
$\epsilon = 2^{-10}, \mu = 2^{-20}$	64	1.7529e-2	3.2922e-2	7.6720e-3
	128	1.1424e-2	1.6041e-2	2.0428e-3
	256	7.0803e-3	7.4631e-3	5.2306e-4
	512	3.8328e-3	3.7290e-3	1.3169e-4
	1024	1.9825e-3	1.9649e-3	3.3024e-5
	2048	1.0069e-3	1.0063e-3	8.2656e-6

An exact solution and DEFOM numerical solution of example 7.1 is depicted in **Figure 1** for several values of μ. This figure demonstrates that the DEFOM effectively aligns with the exact solution. The computational solution of example 7.2, with a fixed ϵ and varying μ values, as well as a fixed μ and varying ϵ, is illustrated in **Figure 2**. This graphic illustrates that layer behaviors alter with varying parameters, particularly when the μ values are reduced, resulting in a strong appearance of the right-side layer. **Figure 3** also illustrates the MFDM numerical solution with the exact solution for various values of μ. These figures indicate that when ϵ declines, a boundary layer exists, if μ is tiny, the boundary layer is presented near $x = 0$ and $x = 1$, wherever $\epsilon \ll \mu^2$ then the layer shown only around $x = 0$. The numerical

calculations of both methods, MFDM, are exactly the same. A comparison of errors graphically using DEFOM and MFDM approaches is showed **Figure 4** and **Figure 5**.

Additionally, **Table 2** and **Table 5** presents a comparison of the error and the convergence rate of DEFOM and MFDM for example 7.1 and example 7.2 with a fixed value of $\mu = 2^{-7}$. These tables indicate that the problem behaves like a convection-diffusion type model, resulting in DEFOM exhibiting first-order convergence, whereas MFDM demonstrates second-order convergence. **Table 3** and **Table 6** present a comparison of the error and the convergence rate while maintaining $\epsilon = 2^{-10}$. Altering the μ parameter transforms the one-sided layer into two-sided layers, thus modifying the convergence order from first-order convergence to second-order convergence. **Table 4** and **Table 7** present a comparison of the error for both methodologies, with the minimum value of $\mu = 2^{-20}$. These tables demonstrate that the problem exhibits characteristics similar to a reaction-diffusion model, wherein both methods yield second-order convergence. **Table 8** shows the comparison table with the existing Shishkin mesh scheme and **Table 9** shows the comparison with the standard finite difference method. In both tables indicates that MFDM method yields very efficient results. **Figure 6** and **Figure 7** demonstrate the numerical convergence rate on a log-log scale for graphical illustration.

8. Conclusion

This research compares the numerical computations of the developed exponentially fitted operator method and the monotone finite difference method. A significant utilization of existing methodologies, which effectively provide first and second-order rates of convergence. Our technique incorporated the DEFOM and MFDM for derivatives on uniform meshes, alongside the composite trapezoidal rule applied to an integral segment with a uniform mesh. Establishing the maximum absolute error and the convergence rate of DEFOM and MFDM, followed by an explicit comparison of both methods, is notably novel in this field of study. The significant discoveries and contributions of our studies are:

- Investigating layer behaviors within the solution through DEFOM and MFDM.
- The effective implementation of DEFOM and MFDM for the derivative component and the composite trapezoidal rule utilized for the integral component.
- The comparison of maximum absolute error and the verification of the convergence rate of both methods represent significant accomplishments from previous endeavours.

Conflicts of Interest

The authors declare that they have no conflicts of interest regarding this publication.

Acknowledgments

The authors express their gratitude for the APC funding received from Amrita Vishwa Vidyapeetham, Coimbatore, India.

AI Disclosure

The authors declare that no assistance is taken from generative AI to write this article.

References

Amirali, I., Durmaz, M.E., & Amiraliyev, G.M. (2024). A monotone second-order numerical method for Fredholm integro-differential equation. *Mediterranean Journal of Mathematics*, *21*(7), 198. https://doi.org/10.1007/s00009-024-02746-6.

Amiraliyev, G.M., Durmaz, M.E., & Kudu, M. (2018). Uniform convergence results for singularly perturbed Fredholm integro-differential equation. *Journal of Mathematics and Analysis*, *9*(6), 55-64.

Amiraliyev, G.M., Durmaz, M.E., & Kudu, M. (2020). Fitted second-order numerical method for a singularly perturbed Fredholm integro-differential equation. *Bulletin of the Belgian Mathematical Society Simon Stevin*, *27*(1), 71-88.

Ansari, K.J., Izadi, M., & Noeiaghdam, S. (2024). Enhancing the accuracy and efficiency of two uniformly convergent numerical solvers for singularly perturbed parabolic convection–diffusion–reaction problems with two small parameters. *Demonstratio Mathematica*, *57*(1), 20230144. https://doi.org/10.1515/dema-2023-0144.

Chow, J.H., Allemong, J.J., & Kokotovic, P.V. (1978). Singular perturbation analysis of systems with sustained high frequency oscillations. *Automatica*, *14*(3), 271-279.

Cimen, E., & Cakir, M. (2021). A uniform numerical method for solving singularly perturbed Fredholm integro-differential problem. *Computational and Applied Mathematics*, *40*(2), 42. https://doi.org/10.1007/s40314-021-01412-x.

Deepika, P., & Das, A. (2024). A robust numerical scheme via grid equidistribution for singularly perturbed delay partial differential equations arising in control theory. *International Journal of Applied and Computational Mathematics*, *10*(2), 72. https://doi.org/10.1007/s40819-024-01716-6.

Durmaz, M.E., & Amiraliyev, G.M. (2021). A robust numerical method for a singularly perturbed Fredholm integro-differential equation. *Mediterranean Journal of Mathematics*, *18*(24), 1-17.

Durmaz, M.E., Cakir, M., Amirali, I., & Amiraliyev, G.M. (2022). Numerical solution of singularly perturbed Fredholm integro-differential equations by homogeneous second order difference method. *Journal Of Computational and Applied Mathematics*, *412*, 114327. https://doi.org/10.1016/j.cam.2022.114327.

Elango, S., Govindarao, L., & Vadivel, R. (2025). A comparative study on numerical methods for Fredholm integro-differential equations of convection-diffusion problem with integral boundary conditions. *Applied Numerical Mathematics*, *207*, 323-338.

Elango, S., Govindarao, L., Mohapatra, J., Vadivel, R., & Hu, N.-T. (2024). Numerical analysis for second order differential equation of reaction-diffusion problems in viscoelasticity. *Alexandria Engineering Journal*, *92*, 92-101.

Govindarao, L., & Sekar, E. (2023). B-spline method for second order RLC closed series circuit with small inductance value. In *Journal of Physics: Conference Series* (Vol. 2646, No. 1, p. 012039). IOP Publishing. Oxford, UK.

Govindarao, L., Ramos, H., & Elango, S. (2024). Numerical scheme for singularly perturbed Fredholm integro-differential equations with non-local boundary conditions. *Computational and Applied Mathematics*, *43*(3), 126. https://doi.org/10.1007/s40314-024-02636-3.

Hu, N.-T., Elango, S., Chen, C.-S., & Manigandan, M. (2024). Computational methods for singularly perturbed differential equations with the advanced argument of convection-diffusion type. *AIMS Mathematics*, *9*(8), 22547-22564.

Izadi, M., & Kamandar, M. (2025). Fractional-order Liouville–Caputo electrical circuit models: QLM-Dickson matrix collocation algorithms. *Computers and Electrical Engineering*, *122*, 109981. https://doi.org/10.1016/j.compeleceng.2024.109981.

Izadi, M., & Yuzbasi, S. (2022). A hybrid approximation scheme for 1-D singularly perturbed parabolic convection-diffusion problems. *Mathematical Communications*, *27*(1), 47-62.

Izadi, M., Srivastava, H.M., & Kamandar, M. (2025). The LDG finite-element method for multi-order FDEs: Applications to circuit equations. *Fractal and Fractional*, *9*(4), 230. https://doi.org/10.3390/fractalfract9040230.

Jalilian, R., & Tahernezhad, T. (2019). Exponential spline method for approximation solution of Fredholm integro-differential equation. *International Journal of Computer Mathematics*, *97*(4), 791-801.

Karaaslan, M.F. (2021). Performance assessment of an HDG method for second-order Fredholm integro-differential equation: Existence–uniqueness and approximation. *Turkish Journal of Mathematics*, *45*, 2269-2281.

Kress, R. (1998). Integral equations. In: Kress, R. (ed) *Numerical Analysis* (pp. 287-316). Springer, New York.

Lange, C.G., & Smith, D.R. (1993). Singular perturbation analysis of integral equations. *Studies in Applied Mathematics*, *90*(1), 1-74.

Miller, J.J., O'riordan, E., & Shishkin, G.I. (1996). *Fitted numerical methods for singular perturbation problems: error estimates in the maximum norm for linear problems in one and two dimensions*. World scientific. London.

Mohapatra, J., Priyadarshana, S., & Reddy, N.R. (2023). Uniformly convergent computational method for singularly perturbed time delayed parabolic differential-difference equations. *Engineering Computations*, *40*(3), 694-717.

O'malley, R.E. (1967). Two-parameter singular perturbation problems for second-order equations. *Journal of Mathematics and Mechanics*, *16*(10), 1143-1164.

Peponides, G., Kokotovic, P.V., & Chow, J. (1982). Singular perturbations and time scales in nonlinear models of power systems. *IEEE Transactions on Circuits and Systems*, *29*(11), 758-767.

Prince, P.A., Govindarao, L., & Elango, S. (2025a). Non-standard finite difference scheme for system of singularly perturbed Fredholm integro-differential equations. *Journal of Mathematical Modeling*, *13*(4), 865-882.

Prince, P.A., Govindarao, L., & Elango, S. (2025b). Richardson extrapolation for singularly perturbed Fredholm integro-differential equations. *International Journal of Mathematical, Engineering and Management Sciences*, *10*(6), 2023-2039. https://doi.org/10.33889/IJMEMS.2025.10.6.094

Priyadarshana, S., & Mohapatra, J. (2024). An efficient fractional step numerical algorithm for time-delayed singularly perturbed 2D convection-diffusion–reaction problem with two small parameters. *Numerical Algorithms*, *97*(2), 687-726.

Priyadarshana, S., Mohapatra, J., & Ramos, H. (2024). Robust numerical schemes for time delayed singularly perturbed parabolic problems with discontinuous convection and source terms. *Calcolo*, *61*(1), 1. https://doi.org/10.1007/s10092-023-00552-2.

Priyadarshana, S., Padhan, A., & Mohapatra, J. (2025). Adaptive grid based moving mesh algorithms for singularly perturbed second-order Volterra integro differential equations. *Quaestiones Mathematicae*, *48*(7), 1007-1028. https://doi.org/10.2989/16073606.2025.2462939.

Rahman, M. (2007). *Integral equations and their applications*. WIT Press. Boston.

Şevgin, S. (2014). Numerical solution of a singularly perturbed Volterra integro-differential equation. *Advances in Difference Equations*, *2014*(1), 171. https://doi.org/10.1186/1687-1847-2014-171.

Thota, S., Gopisairam, T., & Bikku, T. (2024). Modelling LCR-circuit into Integro-differential equation using variational iteration method and GRU-based recurrent neural network. In *2024 3rd Edition of IEEE Delhi Section Flagship Conference* (pp. 1-6). IEEE. New Delhi, India.

Udupa, M., Saha, S., & Das, A. (2022). Computational analysis of blood flow through stenosed artery under the influence of body acceleration using Shishkin mesh. *International Journal of Applied and Computational Mathematics*, *8*(3), 107. https://doi.org/10.1007/s40819-022-01304-6.